High surface area, nanostructured boehmite and alumina catalysts: Synthesis and application in the sustainable epoxidation of alkenes

Applied Catalysis A, General 571 (2019) 180–187

Contents lists available at ScienceDirect

Applied Catalysis A, General

journal homepage: www.elsevier.com/locate/apcata

High surface area, nanostructured boehmite and alumina catalysts: Synthesis and application in the sustainable epoxidation of alkenes

Warunee Lueangchaichaweng[a], Bhawan Singh[a,b,c], Dalmo Mandelli[c], Wagner A. Carvalho[c], Sonia Fiorilli[d], Paolo P. Pescarmona[b,*]

[a] Centre for Surface Chemistry and Catalysis, KU Leuven, Celestijnenlaan 200F, 3001, Heverlee, Belgium
[b] Chemical Engineering Group, Engineering and Technology Institute Groningen (ENTEG), University of Groningen, Nijenborgh 4, 9747 AG, Groningen, the Netherlands
[c] Centre of Natural and Human Sciences, Federal University of ABC, 166 Santa Adélia Street, Bangu, Santo André, SP, 09210-170, Brazil
[d] Department of Applied Science and Technology, Politecnico di Torino, Corso Duca degli Abruzzi 24, 10129, Torino, Italy

ARTICLE INFO

Keywords:
Aluminium oxide
Boehmite
Nanorods
Heterogeneous catalyst
Epoxidation
Hydrogen peroxide

ABSTRACT

We report a new, straightforward and inexpensive sol-gel route to prepare boehmite nanorods [γ-AlO(OH)-NR] with an average length of 23 nm ± 3 nm, an average diameter of 2 nm ± 0.3 nm and a high specific surface area of 448 m^2/g, as evidenced by TEM and N_2-physisorption, respectively. The boehmite was converted to γ-alumina with preserved nanorod morphology (γ-Al_2O_3-NR) and high surface area upon calcination either at 400 or 600 °C. These nanostructured materials are active and selective heterogeneous catalysts for the epoxidation of alkenes with the environmentally friendly H_2O_2. The best catalyst, γ-Al_2O_3-NR-400, showed to be versatile in the scope of alkenes that could be converted selectively to their epoxide and displayed enhanced reusability compared to previously reported alumina catalysts. Furthermore, the catalytic performance of the material was enhanced by optimising the reaction conditions such as the solvent and the type of hydrogen peroxide source. Under the optimised reaction conditions, the γ-Al_2O_3-NR-400 catalyst displayed 58% cyclooctene oxide yield after 4 h of reaction at 80 °C with full selectivity towards the epoxide product. The correlation between the catalytic activity of these materials and their physicochemical properties such as surface area, hydrophilicity and number and type of acid sites was critically discussed based on a detailed characterisation study.

1. Introduction

One-dimensional nanomaterials such as nanorods and nanowires are of great interest commercially and scientifically. They display larger surface area compared to their counterparts with larger size and can also show unique and improved mechanical [1], magnetic [2] and electronic properties [3]. Aluminas (Al_2O_3) are a class of versatile materials with widespread applications as adsorbents, catalysts and catalyst supports [4,5]. Particularly, γ-Al_2O_3 is one of the most employed supports for heterogeneous industrial catalysts [6]. The asset of alumina include low cost, relatively high surface area and good chemical and thermal stability [7]. Recently, also the aluminium oxyhydroxide known as boehmite [γ-AlO(OH)] has found application as support for platinum-tungsten catalysts active in the hydrogenolysis reaction of glycerol to 1,3-propanediol [8]. Boehmite and γ-Al_2O_3 are closely related, as the latter can be obtained by dehydration of the former upon thermal treatment [9]. Boehmite and alumina themselves have also been reported to be active heterogeneous catalysts in the epoxidation of alkenes with H_2O_2 [10,11], The activity is strongly dependent on the synthesis route used in their preparation [12]. Boehmite and alumina can be prepared by many synthetic routes such as sol-gel [13], hydrothermal [14] and solvothermal methods [15], or by the hydrolysis of aluminium metal [16]. The synthetic parameters involved in sol-gel methods can be tuned, thus allowing a certain degree of control of the structural and textural properties of the resultant aluminum oxide [17]. Also the acidity and hydrophilicity of alumina can be tuned by varying the type of aluminium precursor, the ratio of water to precursor, the pH and the solvent used in the sol-gel synthesis [18]. An important advantage of these low temperature synthesis methods is the tendency to afford materials with large specific surface area [19]. Many efforts have been focused on the preparation of high surface area one-dimensional alumina nanostructures, e.g. by using surfactants or other structure directing agents [20–22], or sophisticated techniques such as chemical etching of porous anodic alumina [23], electrochemical synthesis [24] or normal and lateral stepwise anodisation [25]. However, a straightforward, highly reproducible sol-gel synthesis

* Corresponding author.
E-mail address: p.p.pescarmona@rug.nl (P.P. Pescarmona).

https://doi.org/10.1016/j.apcata.2018.12.017
Received 24 October 2018; Received in revised form 11 December 2018; Accepted 15 December 2018
Available online 17 December 2018

route without employing templating or chelating agents and under mild conditions would still be a rewarding achievement. Therefore, we focussed our attention on the discovery of a sol-gel synthesis procedure that does not require the use of expensive reagents or surfactants, with the goal of providing a simple and efficient approach for the synthesis of nanostructured boehmite and alumina with very high surface areas, a well-defined structure with uniquely small dimensions and a large population of coordinatively unsaturated Al sites at the surface. These physicochemical features would be desirable for application as heterogeneous catalysts for the sustainable epoxidation of alkenes using the environmentally benign aqueous hydrogen peroxide as the oxidant, with the target of providing a cheaper alternative to the highly active and selective gallium oxide nanorods, which represent the state-of-the-art transition-metal-free heterogeneous epoxidation catalyst [26].

2. Experimental

2.1. Synthesis of $Al_2O_3{\cdot}xH_2O$ nanorods

The protocol for the synthesis of boehmite nanorods [γ-AlO(OH)-NR] was developed by adapting the methodology reported by some of us for the synthesis of gallium oxide nanorods [26], and by employing the Al source (aluminium tri-sec-butoxide) that provided an alumina catalyst with optimum epoxidation activity in a previous study [27]. First, aluminium tri-sec-butoxide (1.23 g, 5 mmol) was dissolved by dropwise addition of 2-butanol (1.60 g) within 10 min, and the obtained clear solution was stirred for 30 min. Then, an ammonia solution (25% aqueous ammonium hydroxide) diluted with absolute ethanol (1:1 v/v, ~1.6 mL) was added dropwise until a pH ≈ 9–10 was reached. The white turbid gel was stirred for 1.5 h and then heated at 70 °C for 23 h. The obtained material was aged for 3 days at ambient temperature while stirring. Finally, the white powder was collected by centrifugation, washed at least three times with ethanol and then dried overnight in an oven at 80 °C in air. This protocol for the synthesis of boehmite nanorods is highly reproducible and efficient, leading to a typical yield of approximately 85%, assuming the product formula to be AlO(OH). The synthesis of the γ-alumina nanorods (γ-Al_2O_3-NR-T, where T is the temperature of the thermal treatment expressed in °C) was carried out by thermal treatment of the prepared γ-AlO(OH)-NR in a calcination oven in air at 400 or 600 °C for 10 h (heating rate: 3 °C/min in both cases).

2.2. Characterisation

Powder X-ray diffraction (XRD) patterns were recorded on a STOE Stadi P Combi diffractometer with position sensitive detector (IP PSD) in the region 2θ = 4.26 to 82°, with internal resolution of 0.03°. The measurements were performed in Debye-Scherrer mode at room temperature using $CuK_{\alpha 1}$ radiation (λ = 1.54056 Å, selected by means of a Ge (111) monochromator). The ICDD database was employed to assign the phases identified by XRD.

N_2-physisorption measurements were performed on a Micromeritics Tristar 3000 equipment. The samples were outgassed under reduced pressure for 12 h at 120 °C (heating rate: 10 °C/min) prior to the measurement. The Brunauer-Emmet-Teller (BET) method was applied to calculate the specific surface area [28].

To evaluate the level of hydrophilicity of the synthesised $Al_2O_3{\cdot}xH_2O$ materials, thermogravimetric analyses (TGA) were carried out under N_2 atmosphere with a heating rate of 10 °C/min on a TGA Q500 from TA Instruments. The samples were pre-treated overnight in a desiccator containing a saturated aqueous solution of NH_4Cl to reach the maximum degree of water adsorption. The number of the water molecules adsorbed per nm^2 of surface of the material (n_{H2O}) was estimated from the weight loss between 25 and 150 °C using the following equation [29]:

$$n_{H2O} = \frac{\Delta m}{m_i} \times \frac{N_A}{A_{BET}\, M_{H20}}$$

where Δm is the weight loss between 25 and 150 °C (g); m_i is the initial mass of the sample at 25 °C (g); N_A is the Avogadro constant ($6.022{\cdot}10^{23}\,mol^{-1}$); A_{BET} is the surface area (nm^2/g); M_{H2O} is the molecular mass of water (18.0135 g/mol).

Transmission electron microscopy (TEM) images were obtained on a Philips FEG CM 200 operating at 200 kV. The samples for TEM analysis were prepared by dispersing the solid in few drops of absolute ethanol in an agate mortar followed by deposition on 300 mesh carbon-coated copper grids. For each set of nanorods, ca. 30 particles were counted and measured to determine the nanorod dimensions.

For the Fourier-Transform Infrared (FT-IR) spectroscopy study of adsorbed ammonia, approximately 20 mg of the boehmite or alumina powders were pressed into thin, self-supporting wafers. The FT-IR measurements were performed on a Bruker Tensor 27 spectrometer equipped with a liquid nitrogen-cooled mercury–cadmium–telluride (MCT) detector, operating at $2\,cm^{-1}$ resolution. Pre-treatments were carried out using a standard vacuum frame, in an IR cell equipped with KBr windows. The wafers were outgassed for 1 h at 250 °C before adsorption of ammonia at room temperature (note that this thermal treatment does not affect the boehmite phase in γ-AlO(OH)-NR, as proven by the XRD pattern in Figure S2). Adsorption of ammonia was studied in the pressure range 0.01–20.0 mbar: the reversible fraction of the adsorbate was then removed by prolonged outgassing at room temperature.

2.3. Catalytic tests

The epoxidation reactions were carried out in a multi-well parallel reaction block, equipped with a heating and stirring unit. The liquid reagents and the solvent were dispensed either manually or through fixed metal tips using a Tecan Genesis RSP 100 liquid-handling high-throughput workstation coupled with a personal computer supplied with Gemini software enabling to program the workstation [27]. The catalytic epoxidation reactions were performed by employing: the selected alkene (2 mmol), di-*n*-butyl ether (1 mmol) as GC internal standard, 50 wt% aqueous H_2O_2 (4 mmol), 2.0 g of solvent (i.e. ethyl acetate in most of the cases). First, a solution containing the alkene and the GC internal standard in the solvent was added. Next, the aqueous solution of hydrogen peroxide was added. The reaction mixtures were stirred for 4 h at 800 rpm and 80 °C in capped vials placed in the multi-well reaction block. Selected catalytic tests were performed on three different batches of γ-Al_2O_3-NR-400, and showed high reproducibility of the results (deviation in the epoxide yield value within ± 2%). For these experiments, the average value of the epoxide yield is reported. The studies of the effect of the type of hydrogen peroxide were carried out by comparing the catalyst performance with 50 wt% aqueous H_2O_2 (Aldrich) to that with 70 wt% aqueous H_2O_2 (only available in Brazil, supplied by Solvay for academic research) and 24.5 wt% anhydrous H_2O_2 in ethyl acetate, which was prepared by removing water from the homogeneous solution of 20 mL of 70 wt% aqueous H_2O_2 and 188 mL of ethyl acetate by means of a Dean-Stark trap at 110 °C. Important safety note: the anhydrous solution of hydrogen peroxide in flammable organic solvents should be considered as dangerous and explosive [30]. For safe handling, the preparation should be performed in a fume hood with a properly ventilated preparation set-up to release the oxygen generated by hydrogen peroxide decomposition and the possibly explosive gas mixtures of solvent and oxygen.

Regardless of the type of hydrogen peroxide solution that was employed, the final concentration of H_2O_2 was the same (ca. 5 wt%) in all catalytic tests. The use of much higher concentration of H_2O_2 in combination with relatively high reaction temperature (≥ 80 °C) is not advised for safety reasons, as the rate of decomposition of hydrogen peroxide into oxygen and water increases with rising reaction

temperature, thus increasing the risks of explosions.

Conversion, epoxide yield and selectivity were determined by gas chromatography (GC) analysis on a Finnigan Trace GC Ultra chromatograph from Interscience, equipped with an RTX-5 fused silica column (5 m; 0.1 mm) [31] or on an Agilent 7890 A gas chromatograph, equipped with an HP 5 capillary column (30 m; 0.25 mm). The identification of the by-products of the epoxidation of the various alkenes was performed by gas chromatography-mass spectrometry (GC–MS) on an Agilent 6890 N gas chromatograph coupled to an Agilent 5973 MSD mass 4 spectrometer. The GC was equipped with a WCOT fused silica column (30 m; 0.25 mm) coated with a 0.25 mm thick HP-5 MS film.

For the recycling tests, after the reaction in ethyl acetate at 80 °C for 4 h, the sample was centrifuged for 10 min at 3500 rpm to deposit the solid catalyst. Next, the reaction solution was removed with a pipette, 5 mL of ethanol were added and the sample was stirred for at least 5 min. The sample was again centrifuged to deposit the catalyst and then the supernatant ethanol solution was removed. The washing procedure was repeated three times. Finally, the samples were dried overnight at 120 °C in air and reused in a new catalytic test.

3. Results and discussion

Boehmite nanorods, γ-AlO(OH)-NR, with distinctly small size and high surface area, were synthesised by a straightforward route via a base-catalysed sol-gel method employing aluminium tri-sec-butoxide as precursor. The XRD pattern of the prepared material (Fig. 1a) can be indexed as boehmite phase [γ-AlO(OH)] with orthorhombic structure (JCPDS 021-1307). TEM images reveal that the prepared boehmite displays nanorod morphology with an average length of 23 nm ± 3 nm and an average width of 2 nm ± 0.3 nm (Fig. 2a and Fig. S3a). These images also suggest the possible presence of some nanoflakes with similar dimensionality to the length of the nanorods. The nanostructuring of boehmite led to a material with remarkably high surface area (448 m^2/g), as revealed by N_2 physisorption analysis. The hydrolysis and condensation rates of aluminium precursors are mainly governed by the type of precursor, the solvent, the water content and the pH [32]. Alkoxides are reactive precursors and generally need complex solvent mixtures or chelating agents to control the hydrolysis and condensation rates [17]. In our synthesis protocol, the chosen molar ratios, Al: H_2O:NH_3:2-BuOH = 1: 6.7: 2.4: 7.3, the use of 2-butanol as solvent and the dropwise addition of aqueous ammonia causing a gradual increase in the pH of the solution, are believed to allow the hydrolysis and condensation reactions to occur slowly, thus leading to the formation of

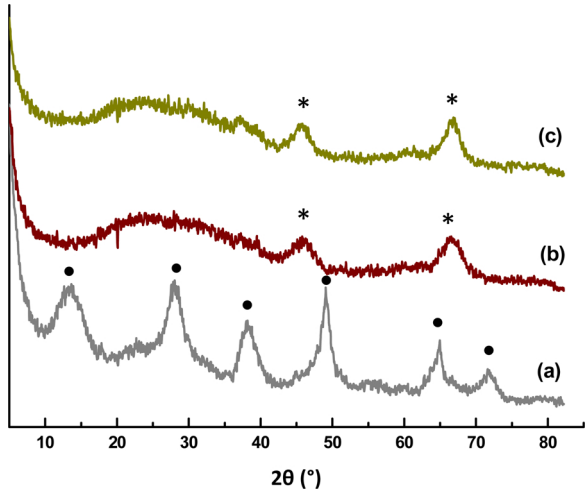

Fig. 1. XRD patterns of (a) as prepared γ-AlO(OH)-NR (b) γ-Al_2O_3-NR-400 and (c) γ-Al_2O_3-NR-600. The circles indicate the position of the diffraction peaks of boehmite; the asterisks denote the position of the diffraction peaks of the (400) and (440) planes of γ-Al_2O_3.

nanorods with small and uniform size and with high surface area [32]. Boehmite has an intrinsic tendency to form in nanorod morphology [33] without need for a structure directing agent. This behaviour is probably related to the orthorhombic crystal lattice of boehmite, in which one cell parameter is much larger than the other two [a = 3.700 Å, b = 12.227 Å, c = 2.868 Å].

The nanostructured boehmite γ-AlO(OH)-NR was converted to γ-Al_2O_3-NR by phase transition induced by calcination, which occurs via the removal of physically- and chemically-bound water. The thermal treatment was carried out either at 400 or 600 °C, and the resulting materials were characterised by XRD, TEM, N_2-physisorption, TGA and FT-IR spectroscopy. Powder XRD analysis (Fig. 1b) showed that the calcination treatment at 400 °C was sufficient to convert the boehmite into a γ-Al_2O_3 phase with tetragonal structure, with the observed broad peaks matching with the JCPDS powder diffraction file 01-074-4629 [34]. The thermal treatment at higher temperature (600 °C, see Fig. 1c) led to a material with the same diffraction pattern, and thus the same structure corresponding to a γ-Al_2O_3 phase. The morphology of the two γ-Al_2O_3 materials was investigated by TEM. The size and morphology of γ-Al_2O_3-NR-400 are very similar to those of the boehmite precursor (Fig. 2b and Fig. S3b), whereas the thermal treatment at 600 °C led to a change in the aspect ratio of the nanorods (width: 3 ± 0.6 nm, length: 13 ± 1 nm). Moreover, particles with less defined morphology are also observed in the latter material (Fig. 2c and Fig. S3c). The phase transition from boehmite to alumina leads to a densification of the materials with a gradual decrease of surface area as a function of increasing calcination temperature. Nevertheless, the surface area of the γ-alumina obtained upon calcination at 400 °C is still remarkably high (376 m^2/g). This high value is ascribed to the small size of these nanorods compared to previous reports of alumina nanorods or nanofibers [35]. The N_2 adsorption/desorption isotherms of the boehmite [γ-AlO(OH)-NR] and of the two γ-Al_2O_3-NR samples (Fig. S1) are of type II according to IUPAC classification, which is typically encountered when adsorption occurs on non-porous materials, in agreement with the open structure of these materials. The hydrophilicity of the materials was estimated by calculating the number of H_2O molecules adsorbed per square nanometre of surface by means of TGA (Table 1). All three materials display similar, relatively low degree of hydrophilicity per surface unit [18,26,36]. This can be explained with their analogous open, non-porous structure, which prevents the entrapment of water molecules that typically occurs in porous aluminas [36]. The materials were further characterised by FT-IR spectroscopy (Fig. 3A). In the high frequency region of the FT-IR spectrum of γ-AlO(OH)-NR outgassed at 250 °C (curve a), the intense bands at 3324 and 3099 cm^{-1} are assigned to the ν_{asym}(Al)O-H and ν_{sym}(Al)O-H stretching vibrations in the boehmite lattice, whereas the narrower band centred at 3668 cm^{-1} is attributed to free or quasi-free surface OH groups [37]. In the low frequency region, the intense band at 1070 cm^{-1} and the shoulder at 1150 cm^{-1} are assigned to the δ_{sym} Al-O-H and δ_{asym} Al-O-H modes of boehmite lattice, respectively [37]. The region below 700 cm^{-1} (not shown) is dominated by the strong stretching mode of 'condensed' AlO_6 octahedra [37]. The two weak bands observed at 2094 and 1973 cm^{-1} can be assigned to combination bands [37]. The OH region of γ-Al_2O_3-NR-400 (curve b) and γ-Al_2O_3-NR-600 (curve c) is markedly different from that shown by γ-AlO(OH)-NR (curve a): the intense bands at 3324 and 3099 cm^{-1} assigned to the stretching vibrations of bulk OH groups disappeared, due to the transformation of the boehmite phase into an alumina phase. In the high frequency region, the intense and broad absorption is attributed to H-bonded surface OH groups, whereas the bands observed at around 3580 cm^{-1}, 3675 cm^{-1} and the shoulder around 3730 cm^{-1} are ascribed to various types of hydroxyls species, differing in the coordination number of the OH group [38]. The weak signals observed in the 1800-1300 cm^{-1} region of all spectra are most likely due to carbonate species formed by the interaction of atmospheric CO_2 with the oxygen atoms of the boehmite and alumina. FT-IR spectroscopy was also used to monitor the adsorption of NH_3 on the

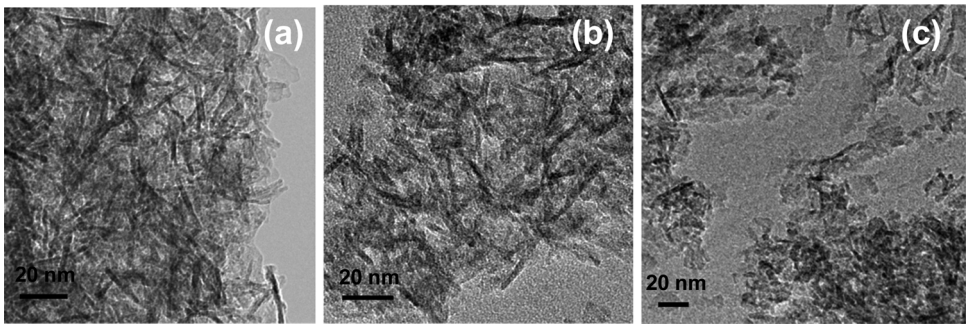

Fig. 2. TEM images of: (a) γ-AlO(OH)-NR, (b) γ-Al_2O_3-NR-400 and (c) γ-Al_2O_3-NR-600.

Table 1
Physicochemical properties and epoxidation activity of the nanostructured boehmite and γ-alumina catalysts and of two types of commercial γ-alumina.

Catalyst	BET surface area (m^2/g)	nH_2O /nm^2 [a]	Dimensions (nm)	Epoxide yield[b,c] (%)			
				Fresh	Rec1	Rec2	Rec3
γ-AlO(OH)-NR	448	9	w: 2 ± 0.3 l: 23 ± 3	29	29	28	27
γ-Al_2O_3-NR-400	376	9	w: 2 ± 0.2 l: 16 ± 1	36	36	33	33
γ-Al_2O_3-NR-600	305	8	w: 3 ± 0.6 l: 13 ± 1	32	33	32	29
Commercial γ-Al_2O_3 [d]	155	–	–	9	–	–	–
Commercial γ-Al_2O_3 nanopowder [e]	171	–	–	16	–	–	–

[a] Estimated by TGA.
[b] Conditions: 2 mmol of *cis*-cyclooctene, 4 mmol of H_2O_2 (as 50 wt% aqueous solution), 40 mg of catalyst, 1 mmol of dibutyl ether (as GC internal standard), 2.0 g of ethyl acetate as solvent, 4 h at 80 °C.
[c] The selectivity towards the epoxide was higher than 99% with all catalysts.
[d] Activated, neutral, Brockmann I, particle size ~150 mesh.
[e] γ-Al_2O_3 nanopowder, particle size < 50 nm (TEM).

surface of the three materials, with the purpose of analysing the type and relative amount of surface acid sites. The difference FT-IR spectra in the low frequency region (the spectrum recorded before ammonia dosage was subtracted for each sample) were obtained after ammonia dosage and upon prolonged outgassing at room temperature (Fig. 3 B). Two positive bands at about 1620 cm^{-1} and 1240 cm^{-1} are irreversibly formed for all three materials and are attributed, respectively, to the anti-symmetric and symmetric bending vibrations of NH_3 coordinated to unsaturated Al^{3+} ions in tetrahedral position, acting as Lewis acid sites [39]. The intensity of these signals is higher for γ-Al_2O_3-NR-400 (curve b), indicating a higher concentration of Lewis acid centres at the surface of this material. The lower intensities observed for γ-AlO(OH)-NR (curve a) and for γ-Al_2O_3-NR-600 (curve c) are ascribable to two different reasons: for the sample treated at 600 °C, the decrease of probed Lewis acid sites is consistent with the observed reduction of surface area upon thermal treatment (Table 1), whereas in the case of the boehmite, the surface is fully hydroxylated, as shown by the related FT-IR spectrum (Fig. 3A.a), thus leading to a relatively low amount of exposed Al (III) cations. The signal at ca. 1465 cm^{-1} is ascribed to the bending vibration of NH_4^+ species formed by proton-transfer reaction with surface hydroxyls, acting as mild Brønsted sites [40] The intensity of the signal is substantially higher for γ-AlO(OH)-NR (a) and γ-Al_2O_3-NR-400 (b) compared to γ-Al_2O_3-NR-600 (c), evidencing a higher concentration of mild Brønsted sites for samples treated at lower temperature, in agreement with their higher population of surface hydroxyl groups.

The physicochemical properties of the prepared nanostructured boehmite and γ-aluminas defined in the characterisation study discussed above are highly attractive for application as catalysts for the epoxidation of alkenes with hydrogen peroxide. Particularly, the nanorod morphology brings about: (i) a high specific surface area; (ii) an open structure with fully accessible surface that intrinsically avoids the diffusion limitations characteristic of high surface area porous catalysts; (iii) a population of surface acid sites that can play a role as active sites; (iv) a relatively low hydrophilicity that can facilitate the approach of the apolar alkene molecules to the catalyst surface and also prevent strong bonding of water, which could poison the active sites [41]. Similar features were identified as the responsible for the notable

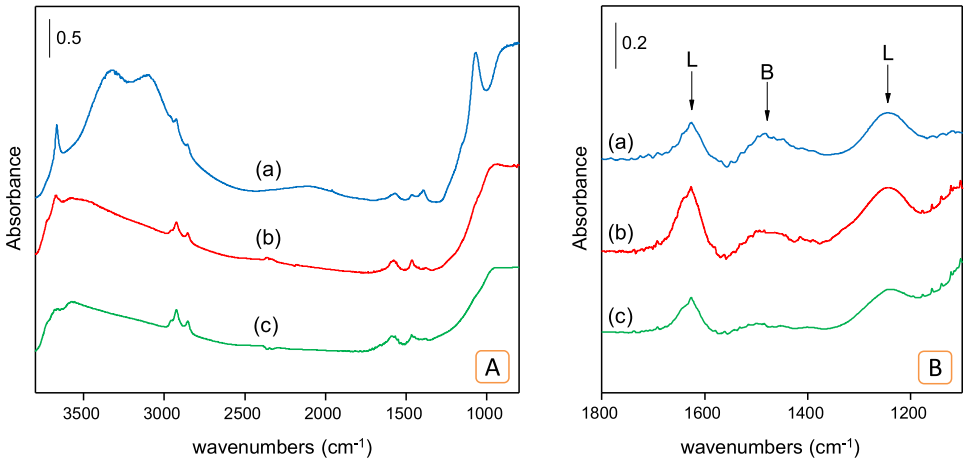

Fig. 3. (A) FT-IR spectra of: (a) γ-AlO(OH)-NR, (b) γ-Al_2O_3-NR-400 and (c) γ-Al_2O_3-NR600, outgassed at 250 °C. (B) FT-IR spectra of: (a) γ-AlO(OH)-NR, (b) γ-Al_2O_3-NR-400 and (c) γ-Al_2O_3-NR600, outgassed at 250 °C and in contact with 20 mbar (equilibrium pressure) of ammonia [L: Lewis acid site; B: Brønsted acid site].

Table 2
Epoxidation of selected alkenes catalysed by γ-Al_2O_3-NR-400 using 50 wt% aqueous H_2O_2 as the oxidant.

Substrate	$Conv_{alkene}$ (%)	$Y_{epoxide}$ (%)	$S_{epoxide}$ (%)	Productivity[a]
Cyclooctene	36	36	> 99	2.3
Cyclohexene	23	23	> 99	1.1
1-Octene	6	6	> 99	0.4
Styrene	19	12	64	0.7
Limonene	42	41[b]	97[b]	3.1

Conditions: 2 mmol of alkene, 4 mmol of H_2O_2 (as 50 wt% aqueous solution), 40 mg of catalyst, 1 mmol of dibutyl ether (as GC internal standard), 2.0 g of ethyl acetate as solvent, 4 h at 80 °C. (Y = yield; S = selectivity).

[a] Productivity is defined as $g_{epoxide}/g_{catalyst}$.

[b] Total epoxides yield and selectivity, the details of the distribution between the internal-, external- and di-epoxides are presented in Fig. 5.

catalytic performance of gallium oxide nanorods [26]. An important asset of this heterogeneous catalyst is the ability to activate hydrogen peroxide towards epoxidation reactions. Aqueous hydrogen peroxide is a highly attractive oxidant for a number of reasons: it is cheap, safely stored and handled, is a mild and an environmentally benign reagent with a high content of active oxygen, and forms water as only by-product. The initial development of transition-metal-free heterogeneous catalysts for epoxidation using aqueous H_2O_2 revolved heavily around metal oxides of group 13. Though their catalytic activity was promising, the poor reusability of the most active among these systems was a main drawback [12,27,42,43]. In this context, a breakthrough was represented by the discovery of gallium oxide nanorods exhibiting significantly enhanced catalytic activity and reusability in the epoxidation reaction [26]. Here, as part of our continued interest in developing this type of catalysts, the nanostructured boehmite [γ-AlO(OH)-NR] and alumina (γ-Al_2O_3-NR-400 and γ-Al_2O_3-NR-600) materials were tested as heterogeneous catalysts for the epoxidation of alkenes with H_2O_2 as the oxidant, with the aim of improving the catalytic performance, especially in term of reusability, compared to previously reported aluminas [10,12,42,43].

In analogy to what has been found for gallium oxide nanorods, the active sites of these nanostructured boehmite and γ-alumina catalysts should be provided by coordinatively unsaturated Al atoms (Lewis acid sites) and mildly acidic surface Al-OH (Brønsted acid sites), which upon interaction with H_2O_2 can form surface hydroperoxide species [26]. For our initial catalytic tests, we choose *cis*-cyclooctene as model substrate and compared the catalytic activity of boehmite and alumina nanorods with two types of commercially available alumina (Table 1). Our boehmite and alumina with nanorod morphology displayed much higher activity compared to the commercial aluminas, while achieving complete selectivity (> 99%) towards the epoxide product in all cases. This confirms the anticipated advantages of the rod-like morphology of our catalysts. The slightly higher activity of γ-Al_2O_3-NR-400 compared to γ-Al_2O_3-NR-600 could be attributed, at least in part, to the larger surface area of the former (Table 1). Nevertheless, γ-AlO(OH) is less active than γ-Al_2O_3-NR-400, despite its larger surface area. Indeed, other factors are known to contribute to the catalytic behaviour of these materials. All of them present an open and accessible surface, thus preventing diffusion limitations during the approach of the reactants to the active site. Moreover, in previous studies of alumina as epoxidation catalysts, it was highlighted that the presence of adsorbed water at the surface of the catalyst is detrimental as it would disfavour the approach of the apolar alkene molecules [36]. The materials reported here display similar, low water-adsorption behaviour (Table 1). These features contribute in explaining the observed promising performance of these catalysts, but still do not account for the observed slightly higher activity of γ-Al_2O_3-NR-400 compared to γ-AlO(OH)-NR. For this purpose, it is necessary to take into account the results of the FT-IR study of the adsorption of NH_3 on the surface of the three catalysts, which indicated that γ-Al_2O_3-NR-400 has similar concentration of Brønsted acid sites and higher concentration of Lewis acid sites compared to γ-AlO(OH)-NR.

Importantly, recycle tests showed that both γ-AlO(OH)-NR and the two γ-Al_2O_3-NR catalysts can be reused in four consecutive runs without significant loss of activity (Table 1). This is a much superior reusability compared to previous reports of the best performing alumina catalysts, whose activity dramatically decreased during successive runs [12,42,43]. This observation is in line with the finding that Ga_2O_3 nanorods show significantly enhanced recyclability compared with previous report on the use of gallium oxides as epoxidation catalysts [26,27,43]. Accordingly, we attribute the excellent reusability of γ-AlO(OH)-NR, γ-Al_2O_3-NR-400 and γ-Al_2O_3-NR-600 to the well-defined structure of the nanorods, providing enhanced chemical stability compared to conventional, unstructured aluminas [12,42,43].

The versatility of the best catalyst for the epoxidation of *cis*-cyclooctene, i.e. γ-Al_2O_3-NR-400, was investigated by expanding the substrate scope to more challenging unsaturated compounds, including a natural product as (R)-(+)-limonene (Table 2). The catalyst was able to convert all tested alkenes, with nearly complete selectivity towards the respective epoxide in the case of cyclooctene, cyclohexene, 1-octene and limonene. This is remarkable particularly in the case of cyclohexene, which is generally prone to undergo side reactions as allylic oxidation or further reaction of cyclohexene oxide to the corresponding diol [44,45]. The high epoxide selectivity obtained here is ascribed to the well-known lack of strong Brønsted acid sites in alumina [46], which implies that ring-opening reactions of the formed epoxide with consequent generation of by-products become unlikely [27]. In the epoxidation of styrene, the selectivity towards styrene oxide was lower (64%) compared to the other epoxides but nevertheless higher compared to state-of-the-art catalysts as gallium oxide nanorods or TS-1 [26]. Benzaldehyde (7% yield), which formed by the oxidative cleavage of the vinyl group of the styrene oxide product [47], was identified as the only side product. The relative activity in the conversion of different alkenes follows the same trend previously observed for gallium oxide nanorods under the same reaction conditions [26] with the latter being consistently more active (both in terms of epoxide yield and productivity). On the other hand, aluminium is a much more abundant and cheaper element compared to gallium (Al is ca. 4000 times more abundant than Ga in the earth crust and ca. 300 times cheaper) [48,49], making this catalyst an attractive alternative for the sustainable epoxidation of alkenes with hydrogen peroxide.

In the case of cyclohexene and limonene, the epoxidation over γ-Al_2O_3-NR-400 was monitored over the course of time. With cyclohexene as substrate, an epoxide of yield of 52% was reached after 28 h (Fig. 4), while retaining a very high selectivity (97%) towards the epoxide with only minor amounts of 2-cyclohexene-1-one and 1,2-cyclohexanediol, thus confirming the very low tendency of this catalyst to promote allylic oxidation or hydrolysis of the epoxide, respectively. The epoxidation of (R)-(+)-limonene was studied in detail because there is growing interest for the utilisation of this bio-based product, which can be obtained from waste peel generated as abundant side product of juice extraction from orange and other citrus fruits [50]. Particularly, the selectivity between the three possible epoxide products (internal-, external- and di-epoxides, see Fig. 5) is worth being studied, as each of these compound can find different applications. For example, the internal limonene oxide has been employed as monomer for copolymerisation with CO_2 to produce fully renewable polycarbonates [51], whereas limonene di-epoxide is used as reactive diluent in cationic UV-curing applications [52] and is employed in the synthesis of limonene dicarbonate, which can be used as monomer for the production of polyurethanes [53]. The internal limonene oxide is the major product throughout the whole reaction (Fig. 5, left plot). The total yield of epoxides reached 78% after 26 h of reaction, with a ratio internal: external: di-epoxide = 90: 7: 3. On the other hand, the selectivity towards the internal epoxide gradually decreased as the reaction proceeded,

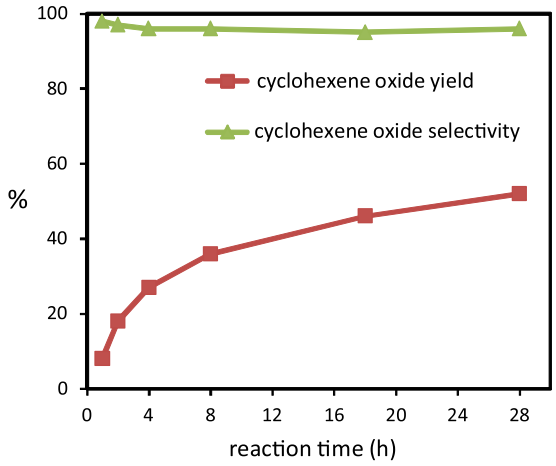

Fig. 4. Kinetic test for the epoxidation of cyclohexene with 50 wt% H_2O_2 catalysed by γ-Al_2O_3-NR-400. Conditions: 2 mmol of cyclohexene, 4 mmol of H_2O_2 (as 50 wt% aqueous solution), 40 mg of catalyst, 1 mmol of dibutyl ether, 2.0 g of ethyl acetate, 4 h at 80 °C.

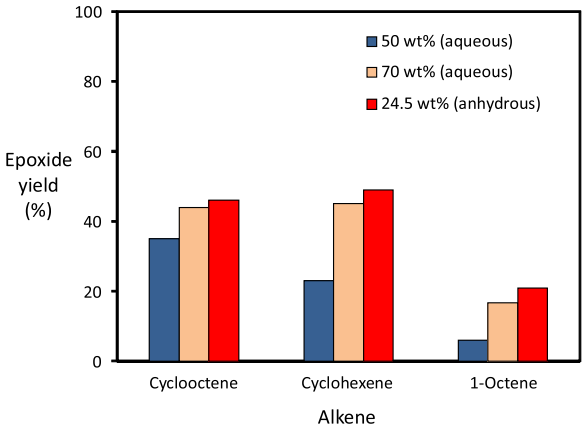

Fig. 6. Effect of the hydrogen peroxide source on the epoxidation of cyclooctene, cyclohexene, and 1-octene using γ-Al_2O_3-NR-400 as catalyst. Conditions: 2 mmol of alkene, 4 mmol of H_2O_2, 40 mg of catalyst, 1 mmol of dibutyl ether, 2.0 g of ethyl acetate, 4 h at 80 °C.

while the selectivity towards the external epoxide, the di-epoxide and the minor side products (mainly diols) gradually increased (Fig. 5, right plot). This indicates that the di-epoxide is mainly formed by further reaction of the internal limonene oxide, which is possibly also more prone to hydrolysis of the epoxide ring with formation of the corresponding diol.

Hydrogen peroxide is generally available as an aqueous solution and in this work most experiments were performed with commercially available 50 wt% aqueous H_2O_2. The nature and amount of solvent in which H_2O_2 is diluted can play an important role on the catalytic performance in epoxidation reactions, as water can compete with hydrogen peroxide for adsorption on the catalyst surface. In this context, it is relevant to investigate the catalytic behaviour of γ-Al_2O_3-NR-400 employing hydrogen peroxide sources with a lower water content, and namely 70 wt% aqueous H_2O_2 and 24.5 wt% anhydrous H_2O_2 in ethyl acetate. This study was carried out on three different substrates: *cis*-cyclooctene, cyclohexene, and 1-octene (Fig. 6 and Table S1). With all the tested alkenes, higher epoxide yields were obtained switching from 50 to 70 wt% aqueous H_2O_2, while retaining analogous very high selectivity towards the epoxide product. A further, though less marked, improvement in epoxide yield was achieved when using the 24.5 wt% anhydrous hydrogen peroxide in ethyl acetate, also in this case without loss of epoxide selectivity. It is worth noting that the increase in epoxide yield was more marked in the epoxidation of cyclohexene and, particularly, 1-octene, reaching more than a two- and three-fold increase, respectively. The enhancement in epoxide yield upon decrease of the water content in the hydrogen peroxide source confirms the detrimental role of water molecules, which can interact with the active sites at the catalyst surface and thus decrease their availability for activating hydrogen peroxide towards the epoxidation reaction [42,54].

Finally, we investigated the effect of the nature of the solvent in which the epoxidation reaction is carried out. The performance of a catalyst in liquid-phase reactions can be strongly influenced by the solvent. Identifying the most suitable solvent can drastically accelerate the rate of reaction, selectivity towards a product, and stability of the catalyst by facilitating the access of the reagents to the active sites of the catalyst and stabilising the transition state [55,56]. When selecting potential solvent candidates, the use of environmentally friendly compounds with low toxicity is preferred, in accordance with the Green Chemistry principles. Additionally, the solvent should be an

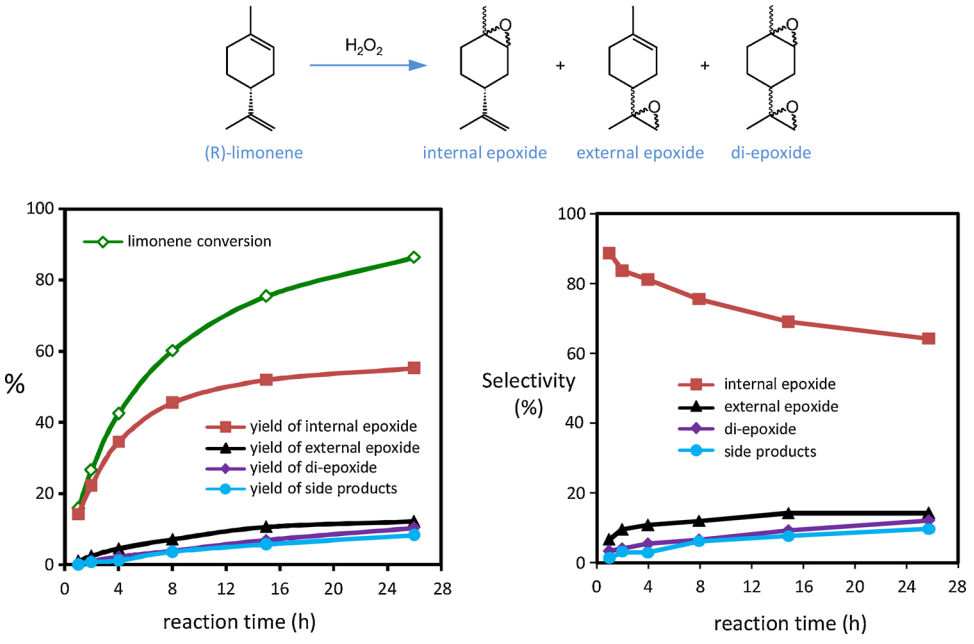

Fig. 5. Kinetic test for the epoxidation of (R)-(+)-limonene with 50 wt% H_2O_2 catalysed by γ-Al_2O_3-NR-400. Conditions: 2 mmol of (R)-(+)-limonene, 4 mmol of H_2O_2 (as 50 wt% aqueous solution), 40 mg of catalyst, 1 mmol of dibutyl ether, 2.0 g of ethyl acetate, 4 h at 80 °C. The ratio between the *cis* and *trans* isomers was estimated to be 1:1.1 for the internal epoxide and 1:1.2 for the external epoxide. For the di-epoxide, the GC peaks were not sufficiently resolved to allow quantification of the RSS:SRS:RSR:SRR ratio. The yields reported in the figure are the sum of the yields of the isomers.

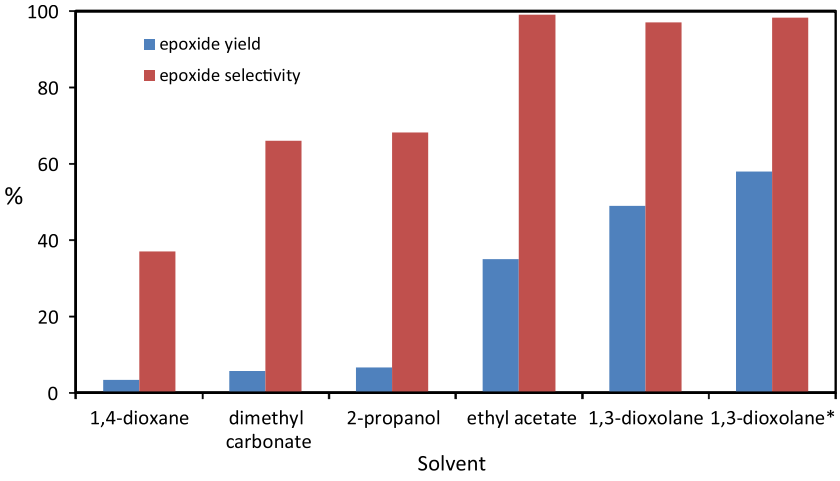

Fig. 7. Effect of the nature of the solvent on the epoxidation of *cis*-cyclooctene with 50 wt% aqueous H_2O_2 using γ-Al_2O_3-NR-400 as catalyst. Conditions: 2 mmol of alkene, 4 mmol of H_2O_2, 40 mg of catalyst, 1 mmol of dibutyl ether, 2.0 g of solvent, 4 h at 80 °C. *Anhydrous H_2O_2 (in ethyl acetate) was used as oxidant instead of 50 wt% aqueous H_2O_2.

inexpensive, available compound. Based on these considerations and taking into account that the solvent should be able to dissolve both the relatively apolar alkenes and the polar hydrogen peroxide, we selected a set of relatively polar green solvents, both protic and aprotic (2-propanol, dimethyl carbonate, 1,4-dioxane and 1,3-dioxolane) and we screened them as alternative to ethyl acetate in the epoxidation of *cis*-cyclooctene with 50 wt% aqueous H_2O_2 over γ-Al_2O_3-NR-400 as catalyst (Fig. 7). Poor epoxide yield and selectivity (with 2-cyclooctene-1-one and 1,2-cyclooctene diol as side products) were observed when 1,4-dioxane, dimethyl carbonate or 2-propanol were employed as solvent. On the other hand, the use of 1,3-dioxolane as solvent led to a significant increase in epoxide yield (49%) compared to ethyl acetate (35%). The yield could be further improved by employing anhydrous hydrogen peroxide instead of the 50 wt% aqueous H_2O_2, reaching 58% cyclooctene oxide yield with nearly full selectivity. The higher activity by using a 1,3-dioxolane as solvent can be ascribed to the observed good dispersion of the catalysts in the monophasic reaction mixture.

4. Conclusions

A facile and cost effective method was developed for the synthesis of high surface area γ-AlO(OH) (boehmite) nanorods, through a very reproducible sol-gel process in which aqueous NH_3 is dosed into a solution of aluminium tri-sec-butoxide in 2-butanol without the need of any structure templating agent or other additive. γ-Al_2O_3 nanorods were obtained through phase transformation upon thermal treatment, which led a slight reduction in specific surface area relative to the as-prepared boehmite nanorods. A characterisation study by means of XRD, TEM, N_2-physisorption, TGA and FT-IR spectroscopy demonstrated that these nanostructured materials display a combination of properties that are suitable for their application as epoxidation catalysts, and namely a high specific surface area, an open, fully accessible structure, a population of surface acid sites, and a relatively low hydrophilicity. Accordingly, the γ-AlO(OH)-NR and γ-Al_2O_3-NR were found to be active and selective heterogeneous catalysts for the epoxidation of alkenes using the environmentally friendly H_2O_2 as the oxidant. The best catalyst, γ-Al_2O_3-NR-400, achieved good activity, excellent selectivity, broad substrate applicability and enhanced reusability compared to previously reported alumina epoxidation catalysts. The superior activity of γ-Al_2O_3-NR-400 is ascribed to the best balance between surface area and nature and concentration of surface acid sites. Furthermore, the activity of γ-Al_2O_3-NR-400 could be substantially enhanced by using anhydrous H_2O_2 instead of 50 wt% aqueous H_2O_2 as the oxidant and by optimising the solvent in which the epoxidation is carried out. Though the maximum achieved activity is still inferior compared to that of previously reported gallium oxide nanorods, which represent the state-of-the-art among transition-metal-free oxide catalysts, these alumina nanorods are a promising alternative considering that aluminium is much more abundant and cheaper than gallium. Additionally, the high surface area and highly accessible open surface of these distinctively small boehmite and γ-alumina nanorods are desirable features for various other catalytic applications, and particularly for the widespread use of aluminas as support for metal nanoparticles [57,58].

Acknowledgements

The authors acknowledge sponsoring in the frame of the following research programs: START1 from KU Leuven (Belgium), project G0D9313N from FWO (Flemish Science Foundation, Belgium) and the related project 490043/2013-5 from CNPq (National Council for Scientific and Technological Development, Brazil). We thank Sonia Parres-Esclapez and Gina Vanbutsele for assistance in the measurement of the N_2-physisorption isotherms. We thank Damiano Cani for the TEM measurements, the Flemish Hercules Stichting for its support in HER/08/25 and the MTM Department for technical support.

Appendix A. Supplementary data

Supplementary material related to this article can be found, in the online version, at doi:https://doi.org/10.1016/j.apcata.2018.12.017.

References

[1] P.E. Marszalek, W.J. Greenleaf, H. Li, A.F. Oberhauser, J.M. Fernandez, Proc. Natl. Acad. Sci. U. S. A. 97 (2000) 6282–6286.
[2] T. Thurn-Albrecht, J. Schotter, G.A. Kastle, N. Emley, T. Shibauchi, L. Krusin-Elbaum, K. Guarini, C.T. Black, M.T. Tuominen, T.P. Russell, Science 290 (2000) 2126–2129.
[3] L. Li, J. Hu, W. Yang, A.P. Alivisatos, Nano Lett. 1 (2001) 349–351.
[4] M.G. Ma, Y.J. Zhu, Z.-L. Xu, Mater. Lett. 61 (2007) 1812–1815.
[5] D.F. Swearer, R.K. Leary, R. Newell, S. Yazdi, H. Robatjazi, Y. Zhang, D. Renard, P. Nordlander, P.A. Midgley, N.J. Halas, E. Ring, ACS Nano 11 (2017) 10281–10288.
[6] (a) J.H. Kwak, J. Hu, D. Mei, C.-W. Yi, D.H. Kim, C.H.F. Peden, L.F. Allard, J. Szanyi, Science 325 (2009) 1670–1673;
(b) M.W. Small, S.I. Sanchez, L.D. Menard, J.H. Kang, A.I. Frenkel, R.G. Nuzzo, J. Am. Chem. Soc. 133 (2011) 3582–3591.
[7] C. Boissière, L. Nicole, C. Gervais, F. Babonneau, M. Antonietti, H. Amenitsch, C. Sanchez, D. Grosso, Chem. Mater. 18 (2006) 5238–5243.
[8] R. Arundhathi, T. Mizugaki, T. Mitsudome, K. Jitsukawa, K. Kaneda, ChemSusChem 6 (2013) 1345–1347.
[9] X. Krokidis, P. Raybaud, A.-E. Gobichon, B. Rebours, P. Euzen, H. Toulhoat, J. Phys. Chem. B 105 (2001) 5121–5130.
[10] (a) D. Mandelli, M.C.A. van Vliet, R.A. Sheldon, U. Schuchardt, Appl. Catal. A 219 (2001) 209–213;
(b) V.R. Choudhary, N.S. Patil, N.K. Chaudhari, S.K. Bhargava, J. Mol. Catal. A: Chem. 227 (2005) 217–222.
[11] A.J. Bonon, Y.N. Kozlov, J.O. Bahu, R.M. Filho, D. Mandelli, G.B. Shul'pin, J. Catal. 319 (2014) 71–86.
[12] R.G. Cesquini, J.M. de S. e Silva, C.B. Woitiski, D. Mandelli, R. Rinaldi,

U. Schuchardt, Adv. Synth. Catal. 344 (2002) 911–914.
[13] S.M. Kim, Y.J. Lee, K.W. Jun, J.Y. Park, H.S. Potdar, Mater. Chem. Phys. 104 (2007) 56–61.
[14] Y. Li, J. Liu, Z. Jia, Mater. Lett. 60 (2006) 3586–3590.
[15] Z. Gan, G. Ning, Y. Lin, Y. Cong, Mater. Lett. 61 (2007) 3758–3761.
[16] M. Thiruchitrambalam, V.R. Palkar, V. Gopinathan, Mater. Lett. 58 (2004) 3063–3066.
[17] T.F. Baumann, A.E. Gash, S.C. Chinn, A.M. Sawvel, R.S. Maxwell, J.H. Satcher, Chem. Mater. 17 (2004) 395–401.
[18] R. Rinaldi, F.Y. Fujiwara, W. Hölderich, U. Schuchardt, J. Catal. 244 (2006) 92–101.
[19] J. Livage, Catal. Today 41 (1998) 3–19.
[20] M.-G. Ma, Y.-J. Zhu, Z.-L. Xu, Mater. Lett. 61 (2007) 1812–1815.
[21] Q. Zhao, X. Xu, H. Zhang, Y. Chen, J. Xu, D. Yu, Appl. Phys. 79 (2004) 1721–1724.
[22] B.D. Clark, C.R. Jacobson, M. Lou, J. Yang, L. Zhou, S. Gottheim, C.J. DeSantis, P. Nordlander, N.J. Halas, Nano Lett. 18 (2018) 1234–1240.
[23] Z.H. Yuan, H. Huang, S.S. Fan, Adv. Mater. 14 (2002) 303–306.
[24] O. Rabin, P.R. Herz, Y.M. Lin, A.I. Akinwande, S.B. Cronin, M.S. Dresselhaus, Adv. Funct. Mater. 13 (2003) 631–638.
[25] L. Pu, X.M. Bao, J.P. Zou, D. Feng, Angew. Chem. Int. Ed. 40 (2001) 1490–1493.
[26] W. Lueangchaichaweng, N.R. Brooks, S. Fiorilli, E. Gobechiya, K. Lin, L. Li, S. Parres-Esclapez, E. Javon, S. Bals, G. Van Tendeloo, J.A. Martens, C.E.A. Kirschhock, P.A. Jacobs, P.P. Pescarmona, Angew. Chem. Int. Ed. 53 (2014) 1585–1589.
[27] P.P. Pescarmona, K.P.F. Janssen, P.A. Jacobs, Chem. Eur. J. 13 (2007) 6562–6572.
[28] B.C. Lippens, J.H. Deboer, J. Catal. 4 (1965) 319–323.
[29] L. Li, T.I. Korányi, B.F. Sels, P.P. Pescarmona, Green Chem. 14 (2012) 1611–1619.
[30] G.R. Astbury, Org. Process Res. Dev. 6 (2002) 893–895.
[31] P.P. Pescarmona, P.A. Jacobs, Catal. Today 137 (2008) 52–60.
[32] C.J. Brinker, G.W. Scherer, Sol-gel Science: The Physics and Chemistry of Sol-Gel Processing, Elsevier, 1990.
[33] P.A. Buining, C. Pathmamanoharan, J.B.H. Jansen, H.N.W. Lekkerkerker, J. Am. Ceram. Soc. 74 (1991) 1303–1307.
[34] I. Levin, D. Brandon, J. Am. Ceram. Soc. 81 (1998) 1995–2012.
[35] (a) S. Shen, W.K. Ng, L.S.O. Chia, Y. Dong, R.B.H. Tan, Cryst. Growth Des. 12 (2012) 4987–4994;
(b) Q. Yang, Inorg. Mater. 46 (2010) 953–958.
[36] R. Rinaldi, U. Schuchardt, J. Catal. 227 (2004) 109–116.
[37] (a) S. Music, O. Dragcevic, S. Popovic, Mater. Lett. 40 (1999) 269–274;
(b) H. Hou, Y. Xie, Q. Yang, Q.Guo, C. Tan, Nanotechnol 16 (2005) 741–745.
[38] C. Morterra, G. Magnacca, Catal. Today 27 (1996) 497–532.
[39] G. Busca, Catal. Today 41 (1998) 191–206.
[40] M. Piumetti, M. Armandi, E. Garrone, B. Bonelli, Microporous Mesoporous Mater. 164 (2012) 111–119.
[41] R.A. Sheldon, J. Mol. Catal. 7 (1980) 107.
[42] R. Rinaldi, J. Sepúlveda, U. Schuchardt, Adv. Synth. Catal. 346 (2004) 281–285.
[43] G. Stoica, M. Santiago, P.A. Jacobs, J. Pérez-Ramírez, P.P. Pescarmona, Appl. Catal. A Gen. 317 (2009) 43–53.
[44] M. Guidotti, C. Pirovano, N. Ravasio, B. Lázaro, J.M. Fraile, J.A. Mayoral, B. Coq, A. Galarneau, Green Chem. 11 (2009) 1421–1427.
[45] I.W.C.E. Arends, R.A. Sheldon, Topics Catal. 19 (2002) 133–141.
[46] P. Atkins, T. Overton, J. Rourke, M. Weller, F. Armstrong, Shriver and Atkins' Inorganic Chemistry, Oxford University Press, 2010.
[47] V. Hulea, E. Dumitriu, Appl. Catal. A Gen. 277 (2004) 99–106.
[48] Wolfram research, Inc. http://demonstrations.wolfram.com/ChemicalAbundancesAndProperties/, Accessed on 23 August 2018.
[49] Price of elements and their compounds, https://en.wikipedia.org/wiki/Pricesofelementsandtheircompounds, Accessed 23 August 2018.
[50] V. Negro, G. Mancini, B. Ruggeri, D. Fino, Bioresour. Technol. 214 (2016) 806–815.
[51] (a) L. Peña Carrodeguas, J. González-Fabra, F. Castro-Gómez, C. Bo, A.W. Kleij, Chem. Eur. J. 21 (2015) 6115–6122;
(b) C. Li, R.J. Sablong, C.E. Koning, Angew. Chem. Int. Ed. 128 (2016) 11744–11748.
[52] (a) N. Gould, J. Ward, (SERICOLLTD), GB2461624-A; GB2461624-B, (2010);
(b) R.P. Eckberg, (General Electric Co), US4547431-A (1985).
[53] M. Bähr, A. Bitto, R. Mülhaupt, Green Chem. 14 (2012) 1447–1454.
[54] M.C.A. van Vliet, D. Mandelli, I.W.C.E. Arends, U. Schuchardt, R.A. Sheldon, Green Chem. 3 (2001) 243–246.
[55] W. Fan, P. Wu, T. Tatsumi, J. Catal. 256 (2008) 62–73.
[56] R. Turco, C. Pischetola, R. Tesser, S. Andinia, M. Di Serio, RSC Adv. 6 (2016) 31647–31652.
[57] Z. Zhang, R.W. Hicks, T.R. Pauly, T.J. Pinnavaia, J. Am. Chem. Soc. 124 (2002) 1592–1593.
[58] N. Nagaraju, A. Fonseca, Z. Konya, J.B. Nagy, J. Mol. Catal. A: Chem. 181 (2002) 57–62.